Sinking phytoplankton associated with carbon flux in the Atlantic Ocean

Colleen A. Durkin,[a][*][1] Benjamin A. S. Van Mooy,[1] Sonya T. Dyhrman,[2] Ken O. Buesseler[1]
[1]Marine Chemistry and Geochemistry, Woods Hole Oceanographic Institution, Woods Hole, Massachusetts
[2]Department of Earth and Environmental Science, Lamont–Doherty Earth Observatory, Columbia University, Palisades, New York

Abstract

The composition of sinking particles and the mechanisms leading to their transport ultimately control how much carbon is naturally sequestered in the deep ocean by the "biological pump." While detrital particles often contain much of the sinking carbon, sinking of intact phytoplankton cells can also contribute to carbon export, which represents a direct flux of carbon from the atmosphere to the deep ocean by circumventing the surface ocean food web. Phytoplankton that contributed to carbon flux were identified in sinking material collected by short-term sediment trap deployments conducted along a transect off the eastern shore of South America. Particulate organic carbon flux at 125 m depth did not change significantly along the transect. Instead, changes occurred in the composition and association of phytoplankton with detrital particles. The fluxes of diatoms, coccolithophores, dinoflagellates, and nano-sized cells at 125 m were unrelated to the overlying surface population abundances, indicating that functional-group specific transport mechanisms were variable across locations. The dominant export mechanism of phytoplankton at each station was putatively identified by principal component analysis and fell into one of three categories; (1) transport and sinking of individual, viable diatom cells, (2) transport by aggregates and fecal pellets, or (3) enhanced export of coccolithophores through direct settling and/or aggregation.

Sinking particles in the ocean are composed of both organisms (e.g., phytoplankton and zooplankton) and detrital material (e.g., fecal pellets and aggregates). Together these particles contribute to the biological pump: the process by which carbon is exported from the surface ocean, where it is in semi-equilibrium with the atmosphere, and naturally sequestered in the deep ocean (Volk and Hoffert 1985). Estimates of the amount of carbon transported to the deep ocean by sinking particles vary widely (Boyd and Trull 2007; Henson et al. 2011; Siegel et al. 2014), in part because the production of sinking particles depends on complex ecological processes, which yield particles with different carbon content and sinking velocities (De La Rocha and Passow 2007). Resolving the composition of sinking particles and characterizing the ecological processes that produce them is necessary to identify the mechanisms causing variability in carbon export in the ocean.

The composition of sinking particles can affect both the magnitude and efficiency of carbon flux from the surface ocean through the mesopelagic zone and into the deep ocean (Boyd and Newton 1999; Wilson et al. 2008; Wiedmann et al. 2014). Detrital material often composes the largest fraction of sinking particulate organic carbon (POC) (Fowler and Knauer 1986; Guidi et al. 2008b). Several studies have identified changes in the abundance and composition of large fecal pellets and organic aggregates by examining particles individually (Ebersbach and Trull 2008; Guidi et al. 2008a; Wiedmann et al. 2014), and have linked these observations to changes in the magnitude and efficiency (i.e., attenuation with depth) of carbon flux (Wilson et al. 2008; Wiedmann et al. 2014). Depending on the study location and season, either aggregates or fecal pellets can be responsible for similar proportions of carbon flux (Waite and Nodder 2001; Ebersbach and Trull 2008), suggesting that particle identification is important to determine the particular ecological mechanism that drives carbon flux at specific locations and times.

*Correspondence: cdurkin@mlml.calstate.edu

[a]Present address: Moss Landing Marine Laboratories, Moss Landing, California

The composition of the phytoplankton community also affects the magnitude and efficiency of carbon export. Diatoms and coccolithophores may have a strong influence on carbon flux because their biomineral frustules and coccoliths provide ballast that increases the sinking speed of particles (Armstrong et al. 2002; Klaas and Archer 2002). Averaged over many observations, the biomineral produced by coccolithophores, calcium carbonate, has been associated with low carbon flux and high efficiency carbon export whereas the biomineral produced by diatoms, silica, has been linked with high carbon flux and low efficiency carbon export (Armstrong et al. 2002; Klaas and Archer 2002; Lam et al. 2011). However, at any individual time or location, the mechanistic connection between phytoplankton biominerals and particle flux is often inconsistent (Trull et al. 2008), causing some to question the degree to which phytoplankton biominerals control carbon flux (De La Rocha and Passow 2007). The magnitude and efficiency of particle flux at a single location changes seasonally, likely due to changes in the phytoplankton community and the degree of grazing and degradation that occurs before particles sink out of the euphotic zone (Boyd and Newton 1999; Buesseler and Boyd 2009). Identifying how phytoplankton become associated with sinking particles could help explain variability in both the magnitude and efficiency of carbon flux across locations and over time.

Phytoplankton can become associated with sinking particles by three primary mechanisms. The first and most direct mechanism of phytoplankton transport is gravitational settling of individual phytoplankton cells. Phytoplankton tend to sink faster when they experience low nutrient conditions (Smayda 1971; Bienfang et al. 1982), providing a possible adaptive advantage by transporting cells out of unfavorable surface conditions (Smetacek 1985). In several studies, the observed sinking speed of individual cells was not fast enough to effectively transport phytoplankton from the surface ocean (Smayda 1971; Kiørboe et al. 1996; Waite and Nodder 2001), while in other studies individual phytoplankton cells with increased sinking speeds were capable of sinking out of the surface ocean (Waite et al. 1992a,b). It is not clear under what conditions individual settling cells are transported through the water column, but there is increasing evidence that small particles, the size of individual phytoplankton cells, can be a significant component of sinking carbon in the water column (Dall'Olmo and Mork 2014; Durkin et al. 2015; Puigcorbé et al. 2015). Aggregation of phytoplankton cells is a second process that transports phytoplankton out of the surface ocean and is a particularly important mechanism for the transport of small cells like eukaryotic nanoplankton, picoplankton, and cyanobacteria (Waite et al. 2000; Ebersbach et al. 2014). A modeling study indicated that cyanobacteria can export carbon in proportion to their production in the surface, possibly due to the incorporation of cyanobacterial cells into sinking aggregates (Richardson

and Jackson 2007). Observations confirmed that cyanobacteria sink in large aggregates that are rapidly degraded at depth (Waite et al. 2000; Lomas et al. 2010; Lomas and Moran 2011). Aggregation can also be important for the transport of diatoms, and several studies in diatom-dominated environments have found that high magnitude carbon export did not occur until diatoms formed large aggregates (Jackson et al. 2005; Martin et al. 2011). When this occurs, diatom blooms are apparently decoupled from grazing pressure, enabling a pulse of aggregated cells to be rapid transported to the seafloor (Beaulieu 2002). A third mechanism, zooplankton fecal pellets, can also transport phytoplankton cells, and cells may remain intact after passage through the gut and packaging inside the pellet (Silver and Bruland 1981; Fowler and Fisher 1983; Jansen and Bathmann 2007). Each of these mechanisms (direct gravitational settling, aggregation, and packaging inside fecal pellets) can lead to the association of different phytoplankton types with the export flux of sinking organic carbon. Physical mixing is an important mechanism leading to the downward transport of phytoplankton and their associated particles (Gardner et al. 1995; Omand et al. 2015), but these particles must also continue to sink after downward mixing by one of the above described mechanisms if they are to escape being transported back upward during the next mixing event. At any given time or place, phytoplankton may also be transported by a combination of these mechanisms occurring at the same time, or sequentially through the water column. Links between surface primary production, export mechanisms, and sinking carbon flux for different types of phytoplankton are largely unknown.

In this study, we measured the sinking carbon flux on a transect off the eastern shore of South America and identified potential biological mechanisms responsible for the observed fluxes by characterizing the composition of sinking phytoplankton and particles. The goals of this study were to identify phytoplankton types that contribute to carbon export, constrain the mechanisms that lead to the export of phytoplankton and relate these mechanisms to the observed carbon flux across locations.

Methods

Sampling locations and water column properties

Samples were collected during the DeepDOM cruise in the South Atlantic Ocean aboard the R/V *Knorr* along a 8482 km transect from Montevideo, Uruguay to Bridgetown, Barbados from 29 March 2013 to 04 May 2013 (Table 1). Surface water and particle flux samples (described below) were collected from 19 stations, and sinking particle composition was determined at 9 of the 19 stations. Water column properties were determined at each station using a conductivity temperature depth (CTD, Seabird) instrument equipped with a Biospherical QSP-200L4S photosynthetically available light (PAR)

Table 1. The location and timing of sediment trap deployments in the South Atlantic Ocean, mixed-layer (ML) and euphotic zone (EZ) depths, the average particulate organic carbon (POC) flux with the standard deviation of triplicate or range of duplicate samples, particulate inorganic carbon (PIC) flux, and surface nutrient concentrations.

Station	Location	Deployment date	Length (h)	ML (m)	EZ (m)	POC flux replicates	Geltrap	POC flux (mg m^{-2} d^{-1})	PIC flux (mg m^{-2} d^{-1})	NO$_3$	NH$_4$	PO$_4$	Si
2	38° S 44.97° W	29 Mar 2013	34	98	129	3	-	41 ± 8	9.7	0.3	0.03	0.18	1.05
4	31.25° S 41° W	01 Apr 2013	8.5	69	106	3	-	43 ± 19	3.5	0	0.04	0.11	0.83
5	28.24° S 38.5° W	02 Apr 2013	21.5	70	128	3	-	42 ± 20	4.1	0	0.01	0.06	1.06
		02 Apr 2013	25			3	-	51 ± 11	4.0				
7	22.49° S 33.02° W	05 Apr 2013	23	54	117	3	Yes	30 ± 6	1.3	0.53	0.01	0.07	1.91
		06 Apr 2013	24			3	Yes	30 ± 12	1.2				
8	17° S 29° W	09 Apr 2013	10.5	7	143	3	-	19 ± 10	1.7	0	0.04	0.22	0.85
9	13.5° S 27.5° W	11 Apr 2013	15.5	48	135	2	Yes	38 ± 5	3.4	0	0.12	0.16	1.42
10	9.5° S 26° W	12 Apr 2013	13	74	-	2	Yes	46 ± 0.4	4.7	0.05	0.05	0.17	1.33
11	5.7° S 24° W	14 Apr 2013	11.5	72	-	3	-	52 ± 6	4.2	0.03	0.05	0.15	2.32
12	5.7° S 26° W	15 Apr 2013	13.5	68	102	3	Yes	37 ± 10	0.5	0.07	0.12	0.1	3.15
13	5.7° S 29° W	16 Apr 2013	11.5	78	-	3	-	56 ± 12	9.5	0.06	0.01	0.11	0.5
15	2.6° S 28.5° W	18 Apr 2013	30	48	83	3	Yes	34 ± 2	3.9	0.16	0.01	0.12	0.91
		19 Apr 2013	16.5			3	Yes	34 ± 2	3.1				
16	0° N 33.49° W	22 Apr 2013	13	50	-	3	Yes	30 ± 10	12.7	0.01	0	0.11	0.94
17	1.5° N 37° W	23 Apr 2013	15.5	45	82	2	-	39 ± 5	8.1	0.14	0.14	0.12	0.93
18	3.5° N 39° W	25 Apr 2013	14	60	-	2	-	45 ± 6	8.5	0.08	0.03	0.09	1.11
19	5.92° N 41.26° W	26 Apr 2013	26	91	85	2	Yes	49 ± 4	6.5	0.12	0.03	0.11	3.14
		26 Apr 2013	26.5			1	Yes	63	7.4				
20	5.91° N 45° W	28 Apr 2013	17	100	-	2	-	52 ± 11	7.4	0.07	0.02	0.11	1.65
21	6.5° N 48° W	29 Apr 2013	17	138	91	2	Yes	63 ± 2	4.6	0.003	0.02	0.14	1.64
		29 Apr 2013	17.5			1	Yes	26	5.0				
22	8.25° N 50° W	01 May 2013	13.5	78	80	2	-	63 ± 14	17.1	0	0.05	0.14	1.6
23	9.7° N 55.3° W	03 May 2013	28.5	85	82	2	-	41 ± 8	5.7	0.003	0.03	0.09	3.69
		03 May 2013	29			1	Yes	32	5.2				
		04 May 2013	26			1	Yes	43	5.6				
		04 May 2013	26.5			2	-	32 ± 0.3	4.5				

sensor mounted on a rosette with Niskin bottles. The mixed layer depth was defined as the depth when down-cast temperature measurements decreased by more than 0.15°C m^{-1}. The bottom of the euphotic zone was defined as the depth at which PAR equaled 1% of the surface value. PAR data was not available at several stations because all CTD cast depths conducted at these stations were deeper than the sensor's pressure rating (Table 1). The concentrations of macronutrients in seawater collected in Niskin bottles at 5 m were measured on a hybrid Technicon AutoAnalyzerII and

Alpkem RFA300 system at Oregon State University and data was provided by E. Kujawinski and K. Longnecker.

Surface chlorophyll *a* concentrations from satellite data

The mapped, monthly average of chlorophyll *a* (Chl *a*) concentrations for April 2013 was obtained from the MODIS-aqua satellite observations available at http://ocean-data.sci.gsfc.nasa.gov. The HDF4 files made available by NASA were converted into netcdf format using the h4tonccf_nc4 tool in the HDF4 CF tool kit available from the NASA ESDIS project (http://hdfeos.org/software/h4cflib.php). Netcdf files of Chl *a* were visualized in R software (R Development Core Team 2008) using the "oce" and "ncdf4" libraries.

Surface phytoplankton collection and quantification

Seawater was collected from a depth of 5 m in Niskin bottles attached to a CTD rosette. Whole seawater was preserved in 1% gluteraldehyde by adding 2/3 seawater volume to 1/3 volume of 3% gluteraldehyde in 0.2 μm filtered seawater, for a total volume of 450–500 mL. Samples were stored at 4°C until analysis onshore by microscopy. Preserved phytoplankton were settled from samples in a 50 mL Utermöhl chamber for at least 18 h (Hasle 1978). Phytoplankton were identified and counted in 100 fields of view at 400X magnification on a Zeiss Axiovert S100 microscope. Phytoplankton were categorized as diatom, dinoflagellate, or coccolithophore and additionally classified by genus or morphological type when possible. Cells that were approximately 5 μm in size, often with flagella, were categorized as nano cells. Nano cells and dinoflagellates represent a potential mixture of autotrophic, mixotrophic or heterotrophic species. Cell concentrations were calculated based on the fields of view counted and the volume of seawater settled. Triplicate 50 mL sample volumes from one station were settled and counted and the average and standard deviation of cell abundances from three settled samples did not differ from the abundances and counting uncertainty determined from one settled sample. Therefore, all samples were counted once and uncertainty was calculated as the square root of the number of cells counted, assuming a Poisson distribution (Zar 1999).

Sediment trap design and deployment

Surface-tethered, drifting sediment traps were deployed on arrival at a station. Sediment traps consisted of a large, vertically hanging 2 m diameter conical net with a cod end, hereafter referred to as a net trap (Peterson et al. 2005), with an acoustically triggered closing mechanism. The purpose of the net trap was to collect a large quantity of fresh sinking material. To collect sinking particles for quantitative determinations of carbon flux, a metal frame mounted with four collection tubes, similar to a particle interceptor trap (PIT) (Knauer et al. 1979; Karl et al. 1996), was attached to the surface-tethered line 25 m above the net trap. The PIT tubes were 12 cm in diameter and 70 cm in height. The net trap was deployed at 150 m depth and the PIT tubes at 125 m

depth. An 8.8 lb float was attached to the top of the PIT frame to reduce the occurrence of frame tilting during the deployment period. The PIT tubes and net trap were below the depth of the surface mixed layer at all locations except at station 21, which had a mixed layer depth of 138 m (Table 1).

The PIT tubes were prepared prior to deployment as previously described (Durkin et al. 2015). Seawater was collected from a depth of 500 m at stations 1 (36°S, 54°W), 9, 16, and 22 (Table 1) with Niskin bottles attached to the CTD rosette and the water was filtered through a 1 μm filter. To prepare PIT tubes for carbon flux collection, tubes were filled with filtered seawater and a layer of formalin brine (filtered seawater, 0.6 M NaCl, 0.1% formalin, 3 mM borate buffer) was added to the bottom of the tube. To collect individually sinking particles for identification by microscopy, a jar with a thin layer of polyacrylamide gel was added to the bottom of a PIT tube. The polyacrylamide gel was prepared as previously described (Durkin et al. 2015). The PIT tube frame typically contained replicate PIT tubes for carbon flux measurements and one gel trap tube for particle imaging. The number of replicates varied across stations and a gel trap tube was not deployed at every station (Table 1). At stations 7, 15, and 23, two sediment trap arrays were deployed on consecutive days. At stations 19, 21, and 23, two sediment trap arrays were deployed at the same time. Three additional tubes for carbon flux process blanks were prepared at stations 2, 7, and 15 and remained covered and in the dark on the deck of the ship for the duration of the trap deployment. Trap arrays were deployed for 19.5 h on average but varied by station (Table 1).

Analysis of particulate carbon flux

Recovered PIT tubes were allowed to settle on the deck of the ship for at least 1 h, after which the seawater overlying the formalin brine was siphoned out of the tubes using a peristaltic pump. The brine layer was drained from the bottom of the tube through a 350 μm mesh to remove large zooplankton that may have actively entered the trap (i.e., "swimmers"). Screening has been shown to be an effective method of removing swimmers at one location in the Sargasso Sea (Owens et al. 2012), but may have removed aggregates and fecal pellets that were larger than 350 μm at certain locations of this study (Durkin et al. 2015). Particles in the formalin brine layer were collected by vacuum filtration onto a 25 mm diameter pre-combusted glass fiber filter. Filters were stored at −20°C until processing on shore, where they were dried in an oven at 50–60°C. A filtered sample from one replicate tube from each trap was weighed, and cut in half as in prior studies (Lamborg et al. 2008; Trull et al. 2008; Owens et al. 2012). Material appeared to be evenly distributed on the filters. Each half was weighed again to determine the percent of the total particles from that sample contained on each filter half. One filter half and the remaining replicate filters from each trap were pelletized in tin capsules to measure total

particulate carbon. The single remaining filter half from each trap sample was used to measure particulate inorganic carbon (PIC). Total particulate carbon was measured by the UC Davis Stable Isotope Facility on an Elementar elemental analyzer. Particulate inorganic carbon was measured at the Woods Hole Oceanographic Institution by S. Manganini on a UIC coulometer analyzer with an acidification module. To calculate PIC flux, the PIC measurement was first scaled to the percentage of the filter analyzed. The average PIC measured in all process blanks ($n = 3$) was subtracted from the PIC measured in each individual sample. Blank-corrected sample measurements were then divided by the deployment time and the surface area of the trap (0.0113 m^2). Particulate carbon flux was similarly calculated from the total particulate carbon measurements, with the average of nine process blanks subtracted from each particulate carbon measurement. To calculate particulate organic carbon (POC) flux, the PIC flux was subtracted from the total particulate carbon flux. To identify the influence of measuring POC flux at a fixed depth across locations with changing water column properties, the linear correlation between median POC flux at each station vs. mixed layer depth or euphotic zone depth was determined. An analysis of variance (ANOVA) test was used to determine whether significant differences in flux measurements occurred among stations and a post-hoc Tukey's test was used to identify which stations were different from one another using tools in R software.

POC flux measurements were compared with previously published data from this region to determine whether the regional-scale values obtained were influenced by the measurement method or date of observation. Thorium-234 flux data was obtained from the 2011 Dutch GEOTRACES study by Owens et al. (2015), which sampled along a cruise track similar to this study. Sampling stations on the Dutch GEOTRACES cruise were 35–430 km from the nearest sampling stations on the DeepDOM cruise. The particulate C: ^{234}Th at 100 m depth was calculated using the relationship determined in the study by Owens et al. (2015) and was multiplied by reported values of thorium-234 flux at 100 m to calculate particulate carbon flux at 100 m. A 25 m offset in depth and a 2 yr time difference occurs between the particulate carbon flux calculated from the Owens et al. (2015) study and the POC flux measured in this study.

Particle and cell fluxes

Recovered gel traps settled on the deck of the ship for at least 1 h before overlying water was siphoned off using a peristaltic pump and the gel jar removed from the bottom of the tube. The jar was allowed to settle for an additional hour before gently siphoning off the water overlying the gel. Particles were identified and counted onboard the ship with a TS100 Nikon inverted microscope at 100X magnification in 30 fields of view across the diameter of the gel. All focal planes within the gel were observed for each field of view.

Particles were categorized as aggregate or fecal pellet and cells were categorized as diatom, coccolithophore, dinoflagellate, or nano cell. Nano cells were confirmed to be cells at higher magnification (400X) and they were not present in gels that had not been deployed in traps. Similar to the surface plankton quantifications, nano cells and dinoflagellates must be considered as a potential mix of autotrophic, mixotrophic or heterotrophic life strategies because the fraction of cells in each trophic category was not determined. Silicoflagellates and zooplankton (e.g., foraminifera, radiolarians, copepods) were inconsistently observed among stations and always in low abundance when present. These particle types were not included in the analysis because the counting uncertainty was always high due to the low number of cells observed (typically 0–3 cells). Cyanobacteria and picoplankton are likely a component of plankton fluxes but were not included in this analysis because these cells types could not be resolved by the microscopic methods employed herein. However, their contribution to the flux is indirectly included in this study by the observation of aggregates, which likely contain these cell types and are thought to be the main mechanism transporting picoplankton out of the surface (Waite et al. 2000; Lomas and Moran 2011). The fluxes of individual particles and cells were calculated by dividing particle counts by the surface area counted and the deployment time (particles m^{-2} d^{-1} or cells m^{-2} d^{-1}). The particle flux, cell flux, and surface cell abundance measurements were compared pairwise to determine whether any sets of measurements were significantly linearly correlated across the transect.

The turnover rate of phytoplankton in the surface mixed layer due to vertical export was determined by dividing cell fluxes (cells m^{-2} d^{-1}) by their abundance in the surface (cells m^{-3}) integrated over the depth of the mixed-layer (m).

Turnover rate = flux ÷ (abundance × mixed layer depth)

This calculation assumes that the cell abundance measured at 5 m is representative of their abundances throughout the mixed layer, although the distribution may have been heterogeneous. We also assume that the particles collected in the traps are closely related in time and space to the observed surface plankton community. This may be a valid assumption because particles had to sink less than 125 m before reaching the trap, a distance that most sinking particles travel in less than a few days (Trull et al. 2008). However, temporal and spatial offsets between the surface plankton community and sinking particles are possible. Significant differences in the export turnover rates among plankton types were tested by an ANOVA with a post-hoc Tukey's test.

On-deck incubation experiments

On-deck incubation experiments were conducted to assess the viability of sinking phytoplankton. Seawater from depths

of 5 m and 150 m was collected from Niskin bottles attached to the CTD rosette at stations 7, 15, and 23 and was filtered through a 0.2 μm polycarbonate filter. Sediment trap material collected in the net trap at stations 7, 15, and 23 was divided into eight equal parts using a custom sample splitter (Lamborg et al. 2008). Two parts of the divided sediment trap material were separately filtered onto 47 mm diameter, 5 μm polycarbonate filters by gentle vacuum filtration. Material collected on each filter was rinsed into separate bottles with filtered seawater from either 5 m or 150 m. Particles were resuspended in a total volume of 800 mL and divided into 6, 125 mL aliquots in 200 mL translucent polyethylene bottles. Three bottles were covered with black electrical tape to prevent light from entering, resulting in four different experimental treatments; particles in water from 5 m in the light or the dark and particles in water from 150 m in the light or the dark, with three replicate bottles of each treatment. Bottles were incubated in a flow through, deck board incubator shaded with blue film to mimic roughly 30% PAR. Samples were incubated for a period of 3 d (stations 7 and 15) to 3.5 d (station 23) to provide enough time for cells to divide and changes in abundance to be detected, which has previously been observed after about 2 d (Rynearson et al. 2013). Samples were preserved in 1% gluteraldehyde by adding 62.5 mL of 3% gluteraldehyde in filtered seawater to each bottle.

The samples were analyzed on land by settling 50 mL from each bottle in an Utermöhl chamber for at least 18 h. Utermöhl slides were counted on a Zeiss Axiovert S100 microscope and cells were counted at various magnifications and in different numbers of fields of view, depending on the size of the cell, their abundance in the sample, and how much aggregated organic material was on the slide. For incubated samples from station 23, diatoms in dark bottles were counted on the entire slide at 200X magnification. Diatoms in light bottles were counted in 20 fields of view at 400X magnification, except *Coscinodiscus* cells, which were counted on the entire slide. Coccolithophores, dinoflagellates, and nano cells were counted at 400X magnification in 20 fields of view in the light treatment samples and 40 fields of view in the dark treatment samples. For incubated samples from station 15, diatoms were counted on half the slide at 200X magnification and other phytoplankton types were counted at 400X magnification in 20 fields of view in all treatments. For incubated samples from station 7, diatoms, coccolithophores, and dinoflagellates were counted on the entire slide at 200X magnification and nano cells were counted in 20 fields of view at 400X magnification.

The number of coccolithophore and dinoflagellate cells observed in individual bottles was low (often < 5 cells total), necessitating the combination of counts from triplicate incubation bottles to decrease the counting uncertainty, which was the main source of variability for these cell types. Uncertainty of combined triplicate counts was calculated as the square root of the total number of counts. Diatoms and nano cells were more abundant in the samples (always > 20 cells observed, often > 100 cells observed), and thus counting uncertainty was not greater than the estimated abundance. For these phytoplankton types, statistically significant differences between light and dark treatments were assessed among triplicate samples using a *t*-test.

Principal component analysis

The relationships among surface plankton abundance, surface nutrient concentrations, and particle flux composition along the transect was assessed by a principal component analysis (PCA) for the purpose of identifying groups of stations with similar characteristics. The analysis was conducted with data from the nine stations where all of these variables were measured. Carbon flux measurements were not included in the PCA so that the variability and relationships among stations could be related independent of carbon flux. The PCA with scaled measurements was calculated using tools in the "FactoMineR" library for R software. Duplicate gel trap measurements of particle fluxes were available at five of the nine stations assessed by the PCA, and for these stations the averages of the two observations were used in the analysis. To test whether the PCA results were sensitive to variability among gel trap replicates, four random combinations of gel trap data from each station were selected from among the replicates and each unique combination of gel trap observations was included in a separate PCA along with surface nutrients and plankton abundances.

Stations with similar particle characteristics (i.e., grouped together by the PCA) were compared to identify whether these characteristics might influence the export turnover rate of surface populations and POC flux. The number of export turnover rate measurements in one of the three PCA groups was less than 3, causing statistical tests for differences among the three groups to be less robust. Therefore, measurements from the two most similar PCA groups were combined and compared with the remaining group of stations using the Welch's *t*-test; an appropriate test for comparing populations with unequal sample sizes. Compared with export turnover rate, more measurements of POC flux and POC flux anomaly were made per station resulting in a greater number of observations per PCA group ($n = 9$–19 observations), so an ANOVA was instead used to test for statistically significant differences in flux among the three PCA groups.

Results

Change in carbon flux across the transect

Average POC flux varied between 18 mg C m^{-2} d^{-1} and 63 mg C m^{-2} d^{-1} across the transect (Table 1). For the stations where replicate sediment trap deployments were conducted, the standard deviation of POC flux among replicates from the same trap was between 6% and 55% of the mean. This variability among replicate tubes on the same trap was
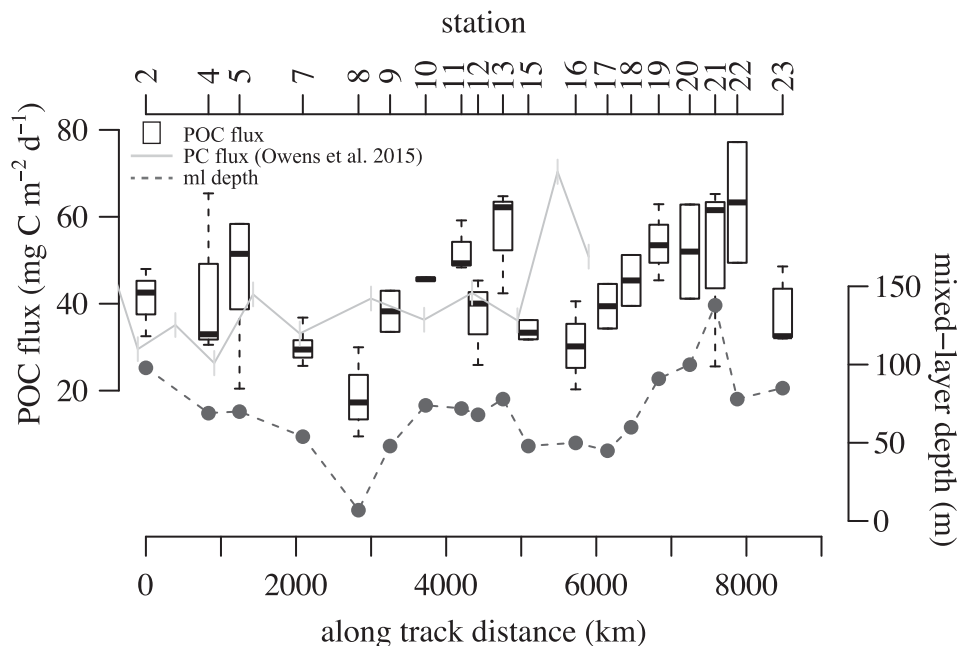
Fig. 1. Measured POC fluxes and water column properties along the DeepDOM transect. Boxplot indicates observed particulate organic carbon (POC) flux at 125 m at locations across the DeepDOM transect. The horizontal line inside the boxes indicates median, the box indicates the first quartiles, and the whiskers indicate 1.5 times the interquartile range. Station ID is indicated along the top axis and corresponding along track distance of the station is indicated along the bottom axis. The light grey line indicates the carbon flux at 100 m calculated from thorium-234 measurements collected during the 2011 Dutch GEOTRACES cruise (Owens et al. 2015). Latitudinal locations from the GEOTRACES cruise were projected onto the along track distance of the DeepDOM cruise. The dashed line indicates mixed-layer depth at each station of the DeepDOM cruise.

greater than or equal to the variability among replicate traps deployed at the same stations (Table 1). For example, at station 5 the standard deviation of POC fluxes collected by replicate tubes on two different traps were 46% and 20% of the average fluxes (Table 1). The average fluxes collected by the two separate traps were 20% different, on par with tube-to-tube variability, and were not significantly different from each other (*t*-test, $p > 0.05$, df = 3). Because the greatest source of variability in the POC flux measurements was between replicate tubes on the same trap, and not among traps at the same station, all replicate POC measurements from the same station were combined (Fig. 1). Significantly different POC fluxes (ANOVA and Tukey's test $p < 0.05$, df = 18) were observed between stations 8 and 11, 8 and 13, 7 and 22, and 8 and 22. The POC fluxes observed in this study were similar in magnitude and spatial variability to the POC fluxes calculated from the thorium-234 flux measured 2 yr previously at 100 m depth (Owens et al. 2015) (Fig. 1).

Spatial variation in POC flux may be caused by changes in the distance between the bottom of the particle production layer and the fixed trap sampling depth: particles may be remineralized to different degrees before being captured in the trap because they sink across variable distances (Buesseler and Boyd 2009). The median POC flux had a significant positive relationship with mixed layer depth across the transect ($r^2 = 0.52$, $p < 0.001$, df = 17, Figs. 1, 2a). Median POC flux was

not related to the euphotic zone depth ($r^2 = 0.18$, $p > 0.05$, df = 17). To remove the influence of changing mixed-layer depth on measured POC fluxes, the POC flux anomaly was determined by subtracting the correlated POC flux value from the measured POC flux values. The POC flux anomaly represents changes in POC flux across the transect that are not related to changes in mixed layer depth, and the median POC flux anomaly varied between -16 mg C m^{-2} d^{-1} and $+18$ mg C m^{-2} d^{-1} (Fig. 2b). The range of POC flux anomalies observed among stations was 26% smaller than the range of POC fluxes observed, and none of the POC flux anomalies were significantly different among stations (ANOVA, $p > 0.05$, df = 18).

PIC flux varied between 0.53 mg C m^{-2} d^{-1} and 17.1 mg C m^{-2} d^{-1} and was significantly, positively correlated with the POC flux measured from the same trap tube ($r^2 = 0.2$, $p < 0.01$, df = 25) but not the POC flux anomaly calculated from the same tube ($r^2 = 0.1$, $p > 0.05$, df = 25) (Table 1). PIC flux was not significantly correlated with mixed-layer depth ($r^2 = 0.05$, $p > 0.05$, df = 17).

Particle and phytoplankton composition across the transect

To investigate changes in the mechanisms leading to carbon flux across the transect, the composition of sinking particles was identified in gel traps at 125 m at nine locations. Particles were composed of aggregates, fecal pellets, nano
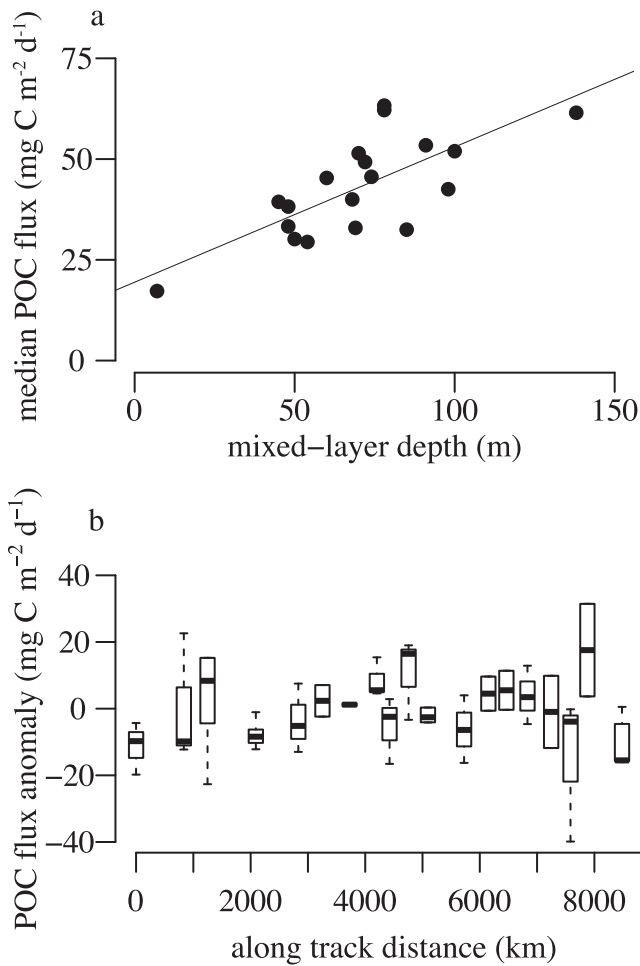
Fig. 2. (**a**) Correlation between median POC flux and mixed-layer depth along the transect ($r^2 = 0.5$). (**b**) Boxplot of the DeepDOM POC flux anomaly when the correlation with mixed-layer depth is removed from each measurement.

cells, dinoflagellates, diatoms, and coccolithophores and the relative abundance of these particle types changed across the transect (Fig. 3). Nano cells were the most consistently numerically abundant particle type observed in the gel traps (29–57% of number flux), followed by aggregates (13–33% of number flux). Fecal pellets and dinoflagellates were less consistently observed and in lower abundance (0–10% of number flux each). Among the other cell-types observed, diatoms contributed 2–34% of the number flux and coccolithophores contributed 3–19% of the number flux. Coccolithophore cell fluxes had no relationship with measured PIC flux ($r^2 = 0.01$, $p > 0.05$, df = 7).

The flux of plankton cells at 125 m was not correlated to the abundance of their surface populations: surface abundances and cell fluxes varied across the transect but not in tandem (Fig. 4). The abundance of dinoflagellates and nano cells varied by twofold across the transect (11–28 cell mL^{-1} and 126–215 cell mL^{-1}, respectively), while their observed

fluxes varied by 65-fold (0.004–0.243 × 10^6 cells m^{-2} d^{-1}) and sixfold (0.396–2.193 × 10^6 cells m^{-2} d^{-1}), respectively. Surface diatom abundance varied 14-fold across the transect (2–21 cell mL^{-1}) and the flux of diatom cells varied 17-fold (0.037–0.627 × 10^6 cells m^{-2} d^{-1}). Surface coccolithophore abundance varied sixfold (3–19 cell mL^{-1}) across the transect excluding station 23, where no coccolithophores were observed, and the flux of coccolithophore cells varied 10-fold (0.046–0.465 × 10^6 cells m^{-2} d^{-1}).

Identifying similar particle flux regimes

To categorize the relationships among plankton cells and sinking particles across the transect, a principal component
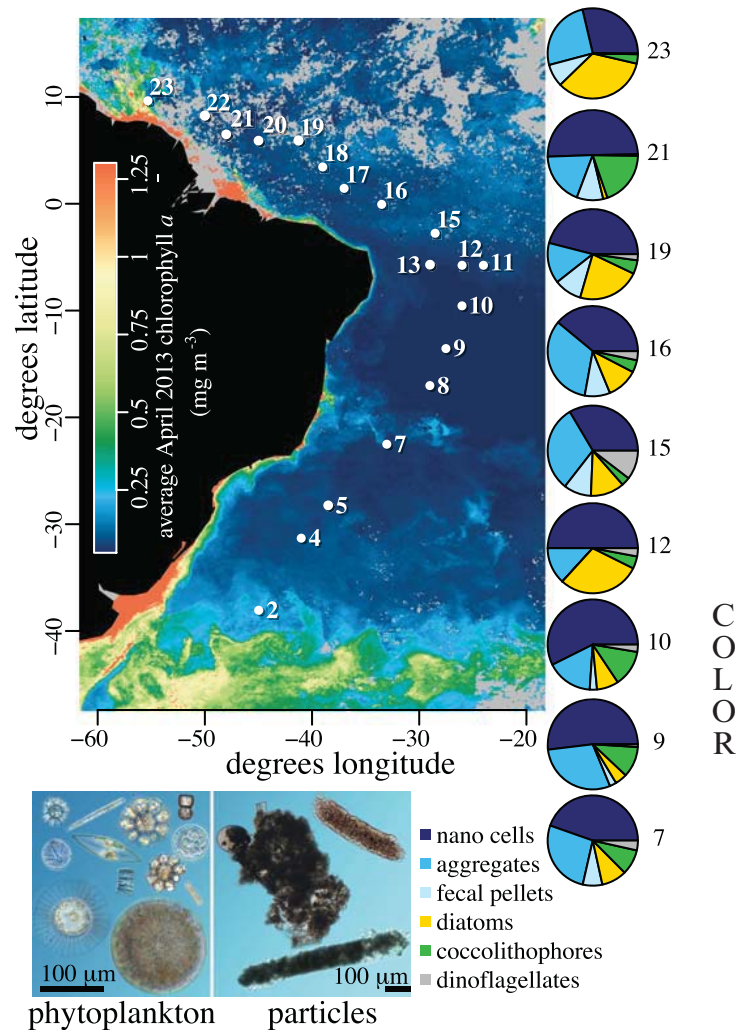

Fig. 3. Sampling locations in the South Atlantic Ocean, overlaid on average Chl *a* concentrations in April 2013 derived from the MODIS-Aqua satellite. Pie charts at right indicate the composition of sinking particles based on numerical abundance at nine locations (station ID indicated at the right of pie chart). The micrograph collage shows example phytoplankton (left side) and particles (right side) in gel trap samples. Particles include diatoms, coccolithophores, fecal pellets, and aggregates. Images of nano cells and dinoflagellates were not available.
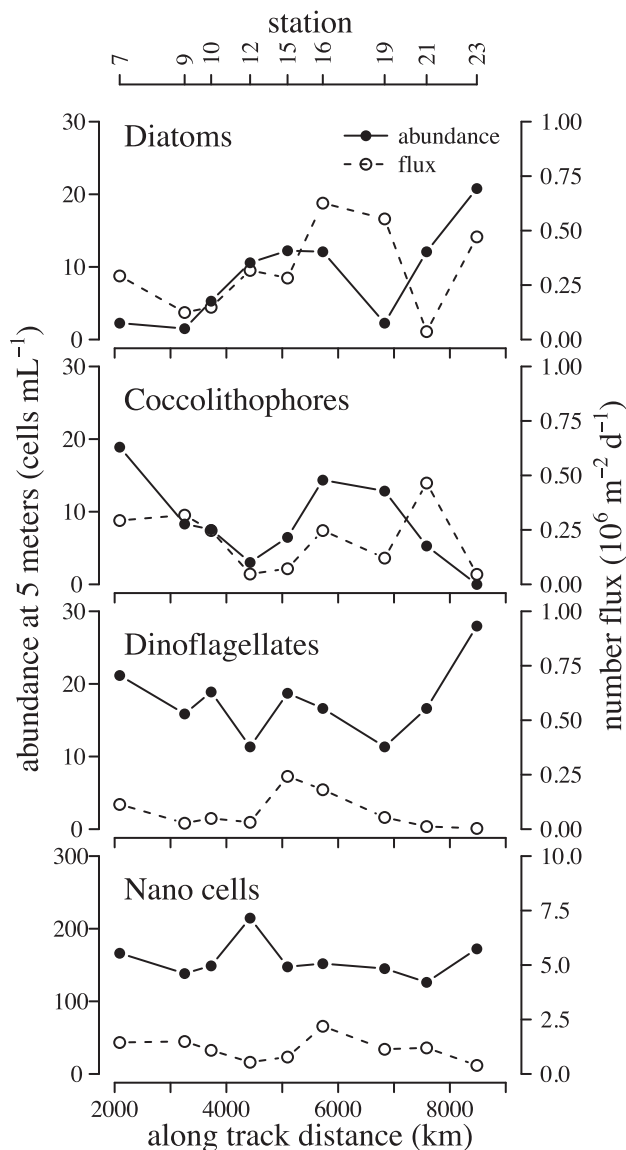
Fig. 4. Abundance at 5 m (solid line) and number flux in gel traps at 125 m (dashed line) of observed phytoplankton types. Data is shown from stations where gel traps were deployed, as indicated along top axis, at locations along the transect, indicated at the bottom axis.

analysis was conducted that included surface nutrient concentrations, surface phytoplankton abundance, and particle number fluxes. The first two principal components of the PCA separated stations into three groups and explained 60% of the total variability (Fig. 5). The first dimension was forced by detrital particles (aggregates and fecal pellets), nano cell flux, dinoflagellate flux, and surface coccolithophores in the positive direction and by mostly diatom-related factors in the negative direction (surface diatoms, surface silicic acid, surface ammonium). The second dimension of the PCA was differentiated by diatom flux in the positive direction and coccolithophore flux and surface phosphate in the negative direction. Stations clus-

tered into three groups; group 1 included stations 12 and 23 and was influenced by diatom-related variables, among others; group 2 included stations 7, 15, 16, and 19, and was located along the dimension most strongly defined by detrital particle flux; group 3 included stations 9,10, and 21 and was defined by coccolithophore flux and surface phosphate and ammonium concentrations. To determine whether the grouping of stations by the PCA was sensitive to the variability in replicate gel trap samples, random combinations of individual observations were included in the PCA instead of the average of replicates (Supporting Information Fig. 1). Stations clustered similarly in each data variation used in the PCA.

Relationship among plankton cells, aggregates, and fecal pellets

The PCA indicated that fecal pellet and aggregate flux had a positive relationship with the flux of dinoflagellates, coccolithophores, and nano cells. The flux of fecal pellets, aggregates, and nano cells co-varied across the transect (Fig. 6a). Nano cell fluxes were positively correlated with the number flux of aggregates ($r^2 = 0.72$, $p < 0.01$, df = 7) (Fig. 6b), and their fluxes were highest at locations in groups 2 and 3 of the PCA. Nano cell fluxes were correlated with fecal pellet number flux ($r^2 = 0.51$, $p < 0.05$, df = 7) across locations (Fig. 6c). No other pairs of measurements in the dataset directly correlated with aggregate number flux or fecal pellet number flux, suggesting that other plankton cell types had more variable relationships with detrital particles across the transect.

Export turnover rate of surface plankton

To determine which environments enhanced the export of each cell type from the surface, the export turnover rate was determined for each PCA group (Fig. 7a). This rate represents the fraction of surface plankton exported out of the mixed layer per day. The range of calculated turnover rates ($3 \times 10^{-3} - 2 \times 10^{-6}$ d^{-1}) indicates that a small fraction of intact cells are lost from the surface due to export, but that fraction can differ by three orders of magnitude depending on the cell type and location. The average export turnover rate of diatoms was 12 times larger than dinoflagellates, and 9 times larger than nano cells (ANOVA and Tukey test, $p < 0.05$, df = 3). The export turnover rate of other cell types averaged across all stations in the transect were not significantly different from one another.

The export turnover rate of surface diatoms had no consistent relationship with the station groupings from the PCA, suggesting that each type of flux environment could export surface diatom populations equally. The export turnover rate of coccolithophores was higher at the stations in PCA group 3 ($n = 3$) compared with the combined turnover rates at stations in PCA groups 1 and 2 ($n = 5$) (Welch t-test, $p < 0.05$, df = 2.6). The export turnover rates of nano cells was higher at group 2 and group 3 stations ($n = 7$) compared with group 1 stations ($n = 2$) (Welch t-test, $p < 0.05$, df = 6.3), but the power of this test is lower because only two observations were available
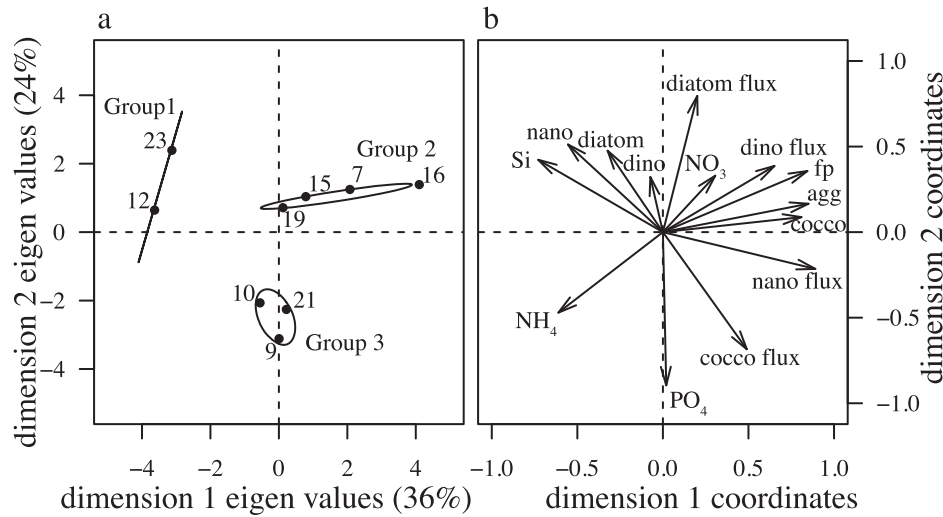
Fig. 5. Principal component analysis of the nine stations where gel traps where deployed, including surface phytoplankton composition, gel trap particle composition, and surface nutrient concentrations as scaled variables. (**a**) Station coordinates plotted by their eigen values and clusters of stations are labeled by group. Circles indicate the 95% confidence interval of station clusters. (**b**) Coordinates of the variable forcing the first and second dimension of the PCA. Labels for variables are as follows: agg (aggregate number flux), cocco (surface coccolithophore abundance), cocco flux (coccolithophore number flux), diatom (surface diatom abundance), diatom flux (diatom number flux), dino (surface dinoflagellate abundance), dino flux (dinoflagellate number flux), fp (fecal pellet number flux), nano (surface nano cell abundance), nano flux (nano cell number flux), and surface dissolved nutrient concentrations of Si, NO_3, NH_4, and PO_4.

from group 1 stations. The export turnover rate of dinoflagellates was not significantly different among stations in different PCA groups (group 2 where $n = 4$ vs. combined groups 1 and 3 where $n = 5$).

The magnitude of POC flux (Fig. 7b) and the POC flux anomaly (excluding the influence of mixed layer depth variability, Fig. 7c) was not significantly different among the three groups of stations identified by the PCA (ANOVA, $p > 0.05$, df = 2), indicating that different flux environments can export similar amounts of POC to 125 m while preferentially exporting different types of phytoplankton.

Viability of sinking phytoplankton cells

Sediment trap material from stations 7, 15, and 23 was incubated on the deck of the ship to identify differences in viability of sinking phytoplankton types. Phytoplankton in the sediment trap material responded similarly when incubated in water collected at 5 m vs. in water collected at 150 m (Table 2). Coccolithophore abundance was low in all incubations (0.05–19 cells mL^{-1}) and did not change in any of the experiments. Dinoflagellate abundance was also low in the incubation experiments (0–10 cells mL^{-1}) and only responded at station 7, where dinoflagellate abundance increased sixfold in water from 5 m and up to 23-fold in water from 150 m when incubated in the light compared with when it was incubated in dark (no dinoflagellates were observed in the corresponding dark incubation, so fold change was calculated assuming that at least one cell was present). The number of cells observed was too small to test whether this response was significant. Nano cells were the

most abundant cell type observed in the incubated material (360–4033 cells mL^{-1}) and at stations 7 and 15 their abundance decreased between 3-fold and 5-fold in light bottles relative to dark bottles in 150 m water (t-test, $p < 0.05$, df = 4). At station 23, nano cell abundance increased threefold in light incubations relative to dark incubations in 5 m water (t-test, $p < 0.05$, df = 4). Diatoms were abundant in incubated material (0.51–1355 cells mL^{-1}) and were significantly more abundant in all light incubations compared with dark incubations (t-test, $p < 0.05$, df = 4). At stations 7 and 15, diatom abundance in light incubations compared with dark incubations increased moderately (3-fold to 7-fold). At station 23, diatoms increased more than 200-fold when incubated in the light compared with the dark.

Overall, little to no change occurred in the abundance of coccolithophores, dinoflagellates, and nano cells when samples were incubated in the light compared with the dark. Diatom abundances also exhibited only small changes in light vs. dark incubations except at station 23. At station 23, diatoms exhibited the largest response of any phytoplankton group in all incubations.

Discussion

Although a similar magnitude of carbon flux from the surface was measured across the entire study region, the particle types responsible for carbon flux changed and the mechanisms leading to particle export also differed among stations. Similar changes in the mechanisms, but not the magnitude, of carbon flux have been observed in a more
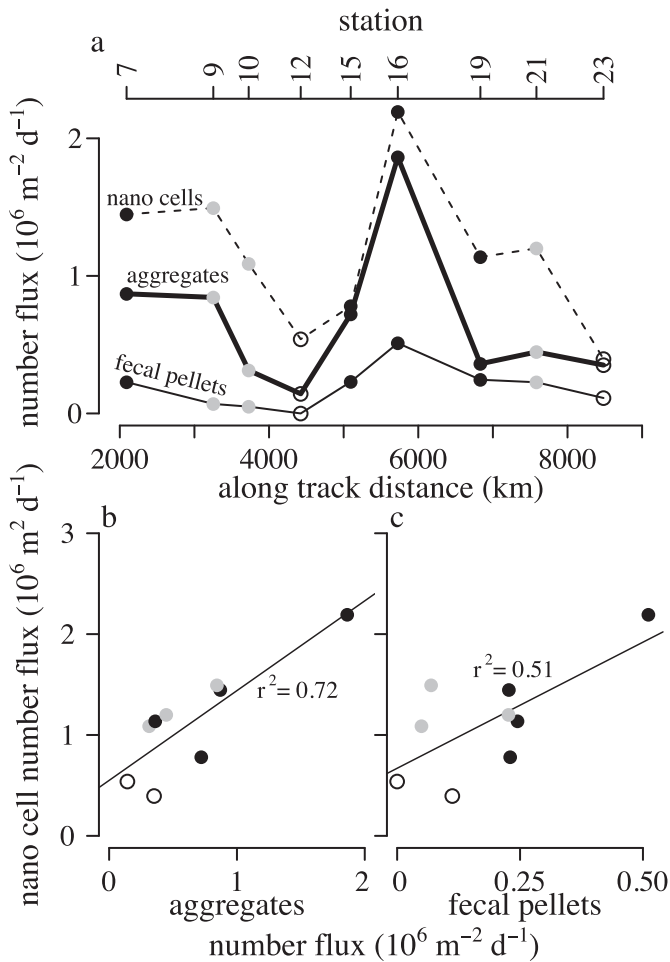
Fig. 6. (**a**) The number flux of aggregates (thick solid line), fecal pellets (thin solid line) and nano cells (dashed line) along the cruise track (bottom axis) at stations where gel traps were deployed (upper axis). Shading of points indicates the PCA grouping of each station; white = PCA group 1, black = PCA group 2, grey = PCA group 3. (**b**) Linear correlation between nano cell flux and aggregate flux. (**c**) Linear correlation between nano cell flux and fecal pellet flux. The correlation coefficients are labeled.

temperate coastal region (Rivkin et al. 1996), suggesting that these finding may be applicable across diverse ocean environments. The changing composition of sinking particles across a region with unchanging carbon flux suggests that variability in the mechanisms of carbon flux might not be reflected in bulk measurements.

The relatively low export turnover rates detected across the transect for all phytoplankton types suggest that only a small fraction of the surface population was transported out of the surface as intact, individual cells, but these data indicate that single cells should be considered an important component of the particle flux. Phytoplankton tend to stay in the surface layer because they can regulate their buoyancy (Gross and Zeuthen 1948) and because turbulent mixing in the surface layer can counter gravitational settling (Huisman

et al. 2002). Observations of phytoplankton cultures show that the majority of cells within a population may sink too slow to be effectively transported out of the surface ocean (< 1–10 m d^{-1}), but that a small fraction of the population may sink almost 10 times faster than the average (Miklasz and Denny 2010). This small fraction of rapidly settling cells may represent an important contribution to export flux. Alternatively, the individual cells observed within the gel traps may be been transported predominantly within aggregates or fecal pellets, which disaggregated at depth. Physical processes may also have transported the small cells and particles observed in this study. All of these processes may have occurred simultaneously, or to different degrees along the transect. In each possible transport scenario, individual particles and cells were at least partially transported by their own sinking velocity because they were collected in the
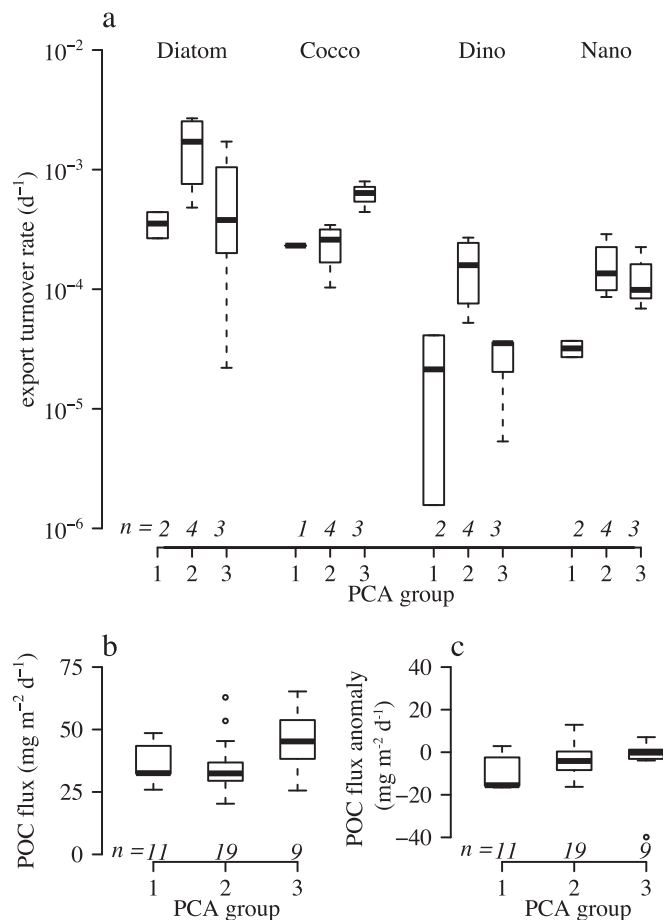

Fig. 7. (**a**) Export turnover rate of each phytoplankton type at combined locations within a PCA grouping. PCA group numbers are indicated along the bottom axis. The number of stations (*n*) with data in each boxplot is indicated above the bottom axis. The *y*-axis is on a log scale due to the difference in scale among phytoplankton types. Coccolithophores were not observed in the surface at station 23 so turnover rate could not be calculated. (**b**) Particulate organic carbon (POC) and (**c**) POC flux anomaly at combined locations of each PCA category.

Table 2. Abundance of phytoplankton cells collected in sediment trap material after incubation in light or dark bottles*.

Cell type	Station	Abundance after incubation (cell mL^{-1})				Fold change	
		5 m dark	5 m light	150 m dark	150 m light	5 m	150 m
Diatom	7	0.7 ± 0.1	2.1 ± 0.1	0.6 ± 0.1	1.6 ± 0.1	3 ± 0.4	3 ± 1
	15	1.8 ± 0.2	10.3 ± 0.5	0.8 ± 0.1	5.6 ± 0.3	6 ± 0.6	7 ± 1
	23	5.2 ± 0.2	1118 ± 74	4.6 ± 0.2	1354 ± 79	216 ± 17	293 ± 22
Coccolithophore	7	0.05 ± 0.02	0.1 ± 0.03	0.07 ± 0.03	0.2 ± 0.05	2 ± 1	3 ± 1
	15	3.8 ± 2.2	6.3 ± 2.8	2.5 ± 1.8	3.8 ± 2.2	2 ± 1	2 ± 1
	23	0.6 ± 0.6	18.9 ± 4.9	1.3 ± 0.9	1.3 ± 1.3	30 ± 31	1 ± 1
Dinoflagellate	7	0.1 ± 0.03	0.6 ± 0.08	0 ± 0	0.2 ± 0.05	6 ± 2	23 ± 5
	15	2.5 ± 1.8	10.1 ± 3.6	1.3 ± 1.3	1.3 ± 1.3	4 ± 3	1 ± 1
	23	1.3 ± 0.9	3.8 ± 2.2	0.6 ± 0.6	5.0 ± 2.5	3 ± 3	8 ± 9
Nano cell	7	2284 ± 54	747 ± 31	2203 ± 53	418 ± 23	0.3 ± 0.02	0.2 ± 0.01
	15	2770 ± 59	2587 ± 57	4033 ± 71	2068 ± 51	0.9 ± 0.03	0.5 ± 0.02
	23	360 ± 15	1002 ± 36	922 ± 24	1094 ± 37	3 ± 0.2	1 ± 0.05

*The counting uncertainty of phytoplankton cells from combined triplicate incubation bottles is reported. When no cells were observed in one of the treatments, the fold change was estimated assuming that at least one cell was present.

bottom of the sediment trap (0.7 m long) and embedded in the gel as distinct, individual particles. Cells would have had to sink between 0.6 m d^{-1} and 1.3 m d^{-1} to settle from the top of the trap tube to the gel layer at the bottom, depending on the deployment time period. Diatom, coccolithophore, and dinoflagellate cultures have been observed to settle at speeds equal to and greater than this range (Smayda 1970; Miklasz and Denny 2010), suggesting that the individual cells observed in the gel trap may have been transported to some degree by there own gravitational settling.

Phytoplankton were transported out of the surface ocean in the South Atlantic by three different export regimes (Fig. 8), defined primarily by station groupings in the principal component analysis. Locations affected by the first plankton export regime (PCA group 1) were characterized by diatom-related factors. Silicic acid levels were high at these locations ($> 3 \mu$M) relative to other locations, enabling the production of an abundant surface diatom population. Number flux of detrital material was low and the flux of diatom cells was high. Grazing and recycling therefore appear to be reduced at these stations relative to the other stations and direct gravitational settling may have had an important role in transporting individual cells. While physical mixing and disaggregation may have also played a role in transporting individual cells through the water column, gravitational settling of diatom cells was necessary to some degree to transport individual cells to the bottom of the gel traps during the deployment period. The sinking speeds of diatoms tend to increase when cells experience physiological stress (Smayda 1971; Bienfang et al. 1982; Waite et al. 1992a), which would increase their likelihood of sinking out of the surface and at a speed rapid enough to be captured in the gel trap. The incubation experiments conducted at station 23 (group 1) suggest that sinking diatoms may have had a different physio-

logical status compared with other locations, as inferred by the increased viability of sinking diatoms in incubated sediment trap material at station 23 compared with other locations. If the physiological status of diatoms at group 1 locations enhanced their sinking speeds, it may have enhanced the transport of individual cells, however the specific nutrient status of surface phytoplankton communities was not evaluated. Alternatively, incubated diatoms may have been subject to less grazing pressure at this location compared with other locations, enabling them to bloom in incubated bottles. Both scenarios suggest that transport was not dominated by grazing food webs at these locations, and instead that individual diatom cells were transported by some other mechanism. Previous studies that integrate flux observations from many times and locations have linked sinking diatoms with high flux, low efficiency export of carbon (Francois et al. 2002; Klaas and Archer 2002). In this study, the carbon flux at diatom-influenced group 1 locations was not higher than at other locations, suggesting that sinking diatoms are not always associated with higher magnitude flux. The mechanisms leading to particle flux at any individual time and location may not be consistent with the patterns determined by averaging across many different observations (Trull et al. 2008; Buesseler and Boyd 2009).

The second phytoplankton export regime (PCA group 2) was defined by the large influence of aggregates and fecal pellets on the transport of phytoplankton cells. Sinking aggregates and fecal pellets are major components of particle flux out of the surface ocean, and were especially influential in transporting small nano cells. The flux of nano cells was directly correlated to the number flux of aggregates at all locations, with the highest flux of both nano cells and aggregates occurring at group 2 locations. The fraction of nano cells exported out of the mixed layer each day (export turnover
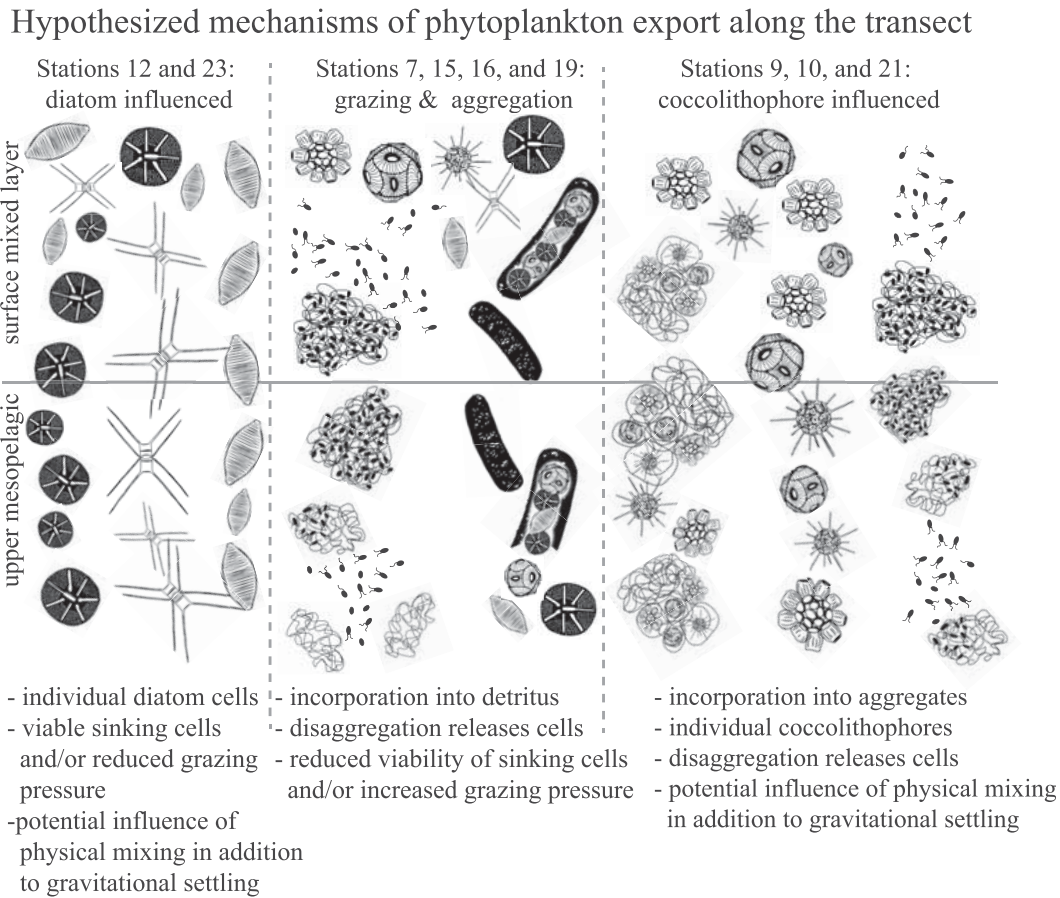
Hypothesized mechanisms of phytoplankton export along the transect

Fig. 8. Schematic of the hypothesized phytoplankton export regimes at stations along the transect. Stations with similar phytoplankton export regimes were identified by grouping together in the PCA (Fig. 5) and further characterized by their shared changes in fecal pellet and aggregate flux (Fig. 6), locations of enhanced export turnover rate (Fig. 7) and response of phytoplankton in incubation experiments (Table 2).

rate) was elevated at group 2 locations, indicating that their incorporation into detrital particles may have enhanced their export at these locations. Ebersbach et al. (2014) similarly found abundant "coccoid cells" in sediment trap material and associated them with transport by aggregates. The nano cells in this study may have been detected as individual cells in the gel trap because they were released when aggregates broke apart prior to collection in the sediment trap. Alternatively, the nano cells could have been responsible for breaking apart aggregates; since the presence of photosynthetic pigments was not determined, it is possible that nano cells were heterotrophic and grazing on the contents of the sinking particles during transport. It is likely that the aggregates were also responsible for the transport of other small phytoplankton that were not quantified in this study, such as cyanobacteria. The flux of diatom and coccolithophore cells was relatively high at group 2 locations, indicating that the detrital material may also have transported these cell types. The reduced viability of incubated cells collected in sediment trap material at group 2 locations suggest that cells may have been partially processed through surface food webs before being transported

out of the surface along with aggregates and fecal pellets, or that grazing was occurring in the trap material itself.

The third phytoplankton export regime (PCA group 3) was defined by enhanced flux of the surface coccolithophore community. The export turnover rate of coccolithophores was relatively high at group 3 locations, indicating that a larger fraction of intact coccolithophores were sinking out of the surface. The export turnover rate of nano cells was also higher at group 3 locations, and these cells were apparently transported by aggregates as described above. Therefore, aggregates were probably an important transport mechanism of coccolithophores at group 3 locations as well. The individual cells observed in the geltraps may have disaggregated before arriving at the trap and sinking into the gel layer. Coccolith production can vary substantially among species and strains of coccolithophores (Young et al. 2005; Langer et al. 2009), and it is possible that differential ballasting of coccolithophore populations may have increased their export turnover rate at group 3 locations relative to other locations. Individual coccolithophore cells may have been more effective at sinking out of the surface layer if their physiological status caused them to sink faster, a response which has been

observed in nitrogen starved laboratory cultures (Lecourt et al. 1996). The combined concentration of nitrate and ammonium was lower than phosphate, creating low surface dissolved N : P ratios at group 3 locations. Coccolithophores may have been nitrogen starved and had enhanced sinking speeds, but their nutrient status at these locations was not evaluated. Previous work has associated the biomineral produced by coccolithophores with low flux, high efficiency export of carbon (Francois et al. 2002; Klaas and Archer 2002; Lam et al. 2011), but coccolithophore-influenced group 3 stations did not have low carbon flux at 125 m. In general, carbon flux was slightly elevated at these locations, although the average is heavily skewed upward by station 21, where sediment trap tubes were within the mixed layer. PIC flux did not correlate with coccolithophore number flux across the transect and PIC flux was also not elevated at group 3 stations. This suggests that the relationship between PIC and carbon flux could reflect the influence of other calcifying organisms (Boyd and Trull 2007), or that the average of regional scale observations do not reflect the mechanisms of flux that occur over short time scales at individual locations.

The three different export regimes identified in this study were all capable of transporting similar amounts of carbon, suggesting that differences in the potential mechanisms of carbon flux may go undetected if only bulk POC flux is observed. Similarly, if particle-focused observational efforts only quantify one process, like aggregation, then equally influential export processes may be overlooked. Individual phytoplankton cells were detected in the gel trap, and may have been transported there by a variety of mechanisms. Since phytoplankton cells quantified in this study were embedded in the gel layer distinctly separated from other particles, they must have moved downward through at least some portion of the water column by themselves. At certain locations, transport via aggregation and fecal pellets appeared to help transport cells through some portion of the water column, but even after cells broke out of aggregates or fecal pellets they continued to move downward into the gel trap. These results reinforce the numerous studies that identify small particles as important components of carbon flux and particle dynamics throughout the water column (Waite et al. 2000; Richardson and Jackson 2007; Alonso-González et al. 2010; Riley et al. 2012; Close et al. 2013; Dall'Olmo and Mork 2014; Durkin et al. 2015; Puigcorbé et al. 2015). The dynamic and diverse processes that lead to the export of phytoplankton cells from the surface have broad biogeochemical and ecological importance, and additional studies are needed to quantify these process on a global scale, and predict how they will change in the future.

References

Alonso-González, I. J., and others. 2010. Role of slowly settling particles in the ocean carbon cycle. Geophys. Res. Lett. **37**: L13608. doi:10.1029/2010GL043827

Armstrong, R. A., C. Lee, J. I. Hedges, S. Honjo, and S. G. Wakeham. 2002. A new, mechanistic model for organic carbon fluxes in the ocean based on the quantitative association of POC with ballast minerals. Deep-Sea Res. Part II Top. Stud. Oceanogr. **49**: 219–236. doi:10.1016/S0967-0645(01)00101-1

Beaulieu, S. 2002. Accumulation and fate of phytodetritus on the sea floor. Oceanogr. Mar. Biol. Annu. Rev. **40**: 171–232. doi:10.1201/9780203180594.ch4

Bienfang, P. K., P. J. Harrison, and L. M. Quarmby. 1982. Sinking rate response to depletion of nitrate, phosphate and silicate in four marine diatoms. Mar. Biol. **67**: 295–302. doi:10.1007/BF00397670

Boyd, P. W., and P. P. Newton. 1999. Does planktonic community structure determine downward particulate organic carbon flux in different oceanic provinces? Deep-Sea Res. Part Oceanogr. Res. Pap. **46**: 63–91. doi:10.1016/S0967-0637(98)00066-1

Boyd, P. W., and T. W. Trull. 2007. Understanding the export of biogenic particles in oceanic waters: Is there consensus? Prog. Oceanogr. **72**: 276–312. doi:10.1016/j.pocean.2006.10.007

Buesseler, K. O., and P. W. Boyd. 2009. Shedding light on processes that control particle export and flux attenuation in the twilight zone of the open ocean. Limnol. Oceanogr. **54**: 1210. doi:10.4319/lo.2009.54.4.1210

Close, H. G., and others. 2013. Export of submicron particulate organic matter to mesopelagic depth in an oligotrophic gyre. Proc. Natl. Acad. Sci. **110**: 12565–12570. doi:10.1073/pnas.1217514110

Dall'Olmo, G., and K. A. Mork. 2014. Carbon export by small particles in the Norwegian Sea. Geophys. Res. Lett. **41**: 2921–2927. doi:10.1002/2014GL059244

De La Rocha, C. L., and U. Passow. 2007. Factors influencing the sinking of POC and the efficiency of the biological carbon pump. Deep-Sea Res. Part II Top. Stud. Oceanogr. **54**: 639–658. doi:10.1016/j.dsr2.2007.01.004

Durkin, C. A., M. L. Estapa, and K. O. Buesseler. 2015. Observations of carbon export by small sinking particles in the upper mesopelagic. Mar. Chem. **175**: 72–81. doi:10.1016/j.marchem.2015.02.011

Ebersbach, F., and T. Trull. 2008. Sinking particle properties from polyacrylamide gels during the KErguelen Ocean and Plateau compared Study (KEOPS): Zooplankton control of carbon export in an area of persistent natural iron inputs in the Southern Ocean. Limnol. Oceanogr. **53**: 212–224. doi:10.4319/lo.2008.53.1.0212

Ebersbach, F., P. Assmy, P. Martin, I. Schulz, S. Wolzenburg, and E.-M. Nöthig. 2014. Particle flux characterisation and sedimentation patterns of protistan plankton during the iron fertilisation experiment LOHAFEX in the Southern Ocean. Deep-Sea Res. Part Oceanogr. Res. Pap. **89**: 94–103. doi:10.1016/j.dsr.2014.04.007

Fowler, S. W., and N. S. Fisher. 1983. Viability of marine phytoplankton in zooplankton fecal pellets. Deep-Sea Res. Part Oceanogr. Res. Pap. **30**: 963–969. doi:10.1016/0198-0149(83)90051-1

Fowler, S. W., and G. A. Knauer. 1986. Role of large particles in the transport of elements and organic compounds through the oceanic water column. Prog. Oceanogr. **16**: 147–194. doi:10.1016/0079-6611(86)90032-7

Francois, R., S. Honjo, R. Krishfield, and S. Manganini. 2002. Factors controlling the flux of organic carbon to the bathypelagic zone of the ocean. Global Biogeochem. Cycles **16**: 34-1–34-20. doi:10.1029/2001GB001722

Gardner, W. D., S. P. Chung, M. J. Richardson, and I. D. Walsh. 1995. The oceanic mixed-layer pump. Deep-Sea Res. Part II Top. Stud. Oceanogr. **42**: 757–775. doi:10.1016/0967-0645(95)00037-Q

Gross, F., and E. Zeuthen. 1948. The buoyancy of plankton diatoms: A problem of cell physiology. Proc. R. Soc. Lond. B Biol. Sci. **135**: 382–389. doi:10.1098/rspb.1948.0017

Guidi, L., G. Gorsky, H. Claustre, J. C. Miquel, M. Picheral, and L. Stemmann. 2008a. Distribution and fluxes of aggregates >100 μm in the upper kilometer of the South-Eastern Pacific. Biogeosciences **5**: 1361–1372. doi:10.5194/bg-5-1361-2008

Guidi, L., G. A. Jackson, L. Stemmann, J. C. Miquel, M. Picheral, and G. Gorsky. 2008b. Relationship between particle size distribution and flux in the mesopelagic zone. Deep-Sea Res. Part Oceanogr. Res. Pap. **55**: 1364–1374. doi:10.1016/j.dsr.2008.05.014

Hasle, G. R. 1978. The inverted-microscope method. *In* Phytoplankton manual. Museum National d'Histoire Natuelle. editor: A. Sournia.

Henson, S. A., R. Sanders, E. Madsen, P. J. Morris, F. Le Moigne, and G. D. Quartly. 2011. A reduced estimate of the strength of the ocean's biological carbon pump. Geophys. Res. Lett. **38**: L04606. doi:10.1029/2011GL046735

Huisman, J., M. Arrayas, U. Ebert, and B. Sommeijer. 2002. How do sinking phytoplankton species manage to persist? Am. Nat. **159**: 245–254. doi:10.1086/338511

Jackson, G. A., A. M. Waite, and P. W. Boyd. 2005. Role of algal aggregation in vertical carbon export during SOIREE and in other low biomass environments. Geophys. Res. Lett. **32**: L13607. doi:10.1029/2005GL023180

Jansen, S., and U. Bathmann. 2007. Algae viability within copepod faecal pellets: Evidence from microscopic examinations. Mar. Ecol. Prog. Ser. **337**: 145–153. doi:10.3354/meps337145

Karl, D. M., J. R. Christian, J. E. Dore, D. V. Hebel, R. M. Letelier, L. M. Tupas, and C. D. Winn. 1996. Seasonal and interannual variability in primary production and particle flux at Station ALOHA. Deep-Sea Res. Part II Top. Stud. Oceanogr. **43**: 539–568. doi:10.1016/0967-0645(96)00002-1

Kiørboe, T., and others. 1996. Sedimentation of phytoplankton during a diatom bloom: Rates and mechanisms. J. Mar. Res. **54**: 1123–1148. doi:10.1357/0022240963213754

Klaas, C., and D. E. Archer. 2002. Association of sinking organic matter with various types of mineral ballast in the deep sea: Implications for the rain ratio. Global Biogeochem. Cycles **16**: 1116. doi:10.1029/2001GB001765

Knauer, G. A., J. H. Martin, and K. W. Bruland. 1979. Fluxes of particulate carbon, nitrogen, and phosphorus in the upper water column of the northeast Pacific. Deep-Sea Res. Part Oceanogr. Res. Pap. **26**: 97–108. doi:10.1016/0198-0149(79)90089-X

Lam, P. J., S. C. Doney, and J. K. B. Bishop. 2011. The dynamic ocean biological pump: Insights from a global compilation of particulate organic carbon, CaCO3, and opal concentration profiles from the mesopelagic. Global Biogeochem. Cycles **25**: GB3009. doi:10.1029/2010GB003868

Lamborg, C. H., and others. 2008. The flux of bio- and lithogenic material associated with sinking particles in the mesopelagic "twilight zone" of the northwest and North Central Pacific Ocean. Underst. Oceans Biol. Pumpresults VERTIGO **55**: 1540–1563. doi:10.1016/j.dsr2.2008.04.011

Langer, G., G. Nehrke, I. Probert, J. Ly, and P. Ziveri. 2009. Strain-specific responses of *Emiliania huxleyi* to changing seawater carbonate chemistry. Biogeosciences **6**: 2637–2646. doi:10.5194/bg-6-2637-2009

Lecourt, M., D. L. Muggli, and P. J. Harrison. 1996. Comparison of growth and sinking rates of non-coccolith- and coccolith-forming strains of *Emiliania huxleyi* (Prymnesiophyceae) grown under different irradiances and nitrogen sources. J. Phycol. **32**: 17–21. doi:10.1111/j.0022-3646.1996.00017.x

Lomas, M., D. Steinberg, T. Dickey, C. Carlson, N. Nelson, R. Condon, and N. Bates. 2010. Increased ocean carbon export in the Sargasso Sea linked to climate variability is countered by its enhanced mesopelagic attenuation. Biogeosciences **7**: 57–70. doi:10.5194/bg-7-57-2010

Lomas, M. W., and S. B. Moran. 2011. Evidence for aggregation and export of cyanobacteria and nano-eukaryotes from the Sargasso Sea euphotic zone. Biogeosciences **8**: 203–216. doi:10.5194/bg-8-203-2011

Martin, P., R. S. Lampitt, M. Jane Perry, R. Sanders, C. Lee, and E. D'Asaro. 2011. Export and mesopelagic particle flux during a North Atlantic spring diatom bloom. Deep-Sea Res. Part Oceanogr. Res. Pap. **58**: 338–349. doi:10.1016/j.dsr.2011.01.006

Miklasz, K. A., and M. W. Denny. 2010. Diatom sinkings speeds: Improved predictions and insight from a modified Stokes' law. Limnol. Oceanogr. **55**: 2513–2525. doi:10.4319/lo.2010.55.6.2513

Omand, M. M., E. A. D'Asaro, C. M. Lee, M. J. Perry, N. Briggs, I. Cetinić, and A. Mahadevan. 2015. Eddy-driven subduction exports particulate organic carbon from the spring bloom. Science **348**: 222–225. doi:10.1126/science.1260062

Owens, S., and others. 2012. A new timeseries of particle export from neutrally buoyant sediment traps at the Bermuda Atlantic Time-series Study site. Deep-Sea Res. Part Oceanogr. Res. Pap. **72**: 34–47. doi:10.1016/j.dsr.2012.10.011

Owens, S. A., S. Pike, and K. O. Buesseler. 2015. Thorium-234 as a tracer of particle dynamics and upper ocean export in the Atlantic Ocean. Deep-Sea Res. Part II Top. Stud. Oceanogr. **116**: 42–59. doi:10.1016/j.dsr2.2014.11.010

Peterson, M. L., S. G. Wakeham, C. Lee, M. A. Askea, and J. C. Miquel. 2005. Novel techniques for collection of sinking particles in the ocean and determining their settling rates. Limnol. Oceanogr.: Methods **3**: 520–532. doi:10.4319/lom.2005.3.520

Puigcorbé, V., and others. 2015. Small phytoplankton drive high summertime carbon and nutrient export in the Gulf of California and Eastern Tropical North Pacific. Global Biogeochem. Cycles **29**: 1309–1332. doi:10.1002/2015GB005134

R Development Core Team. 2008. R: A language and environment for statistical computing, R foundation for statistical computing.

Richardson, T. L., and G. A. Jackson. 2007. Small phytoplankton and carbon export from the surface ocean. Science **315**: 838–840. doi:10.1126/science.1133471

Riley, J. S., R. Sanders, C. Marsay, F. A. C. Le Moigne, E. P. Achterberg, and A. J. Poulton. 2012. The relative contribution of fast and slow sinking particles to ocean carbon export. Global Biogeochem. Cycles **26**: GB1026. doi:10.1029/2011GB004085

Rivkin, R. B., and others. 1996. Vertical flux of biogenic carbon in the ocean: Is there food web control? Science **272**: 1163–1166. doi:10.1126/science.272.5265.1163

Rynearson, T. A., K. Richardson, R. S. Lampitt, M. E. Sieracki, A. J. Poulton, M. M. Lyngsgaard, and M. J. Perry. 2013. Major contribution of diatom resting spores to vertical flux in the sub-polar North Atlantic. Deep-Sea Res. Part Oceanogr. Res. Pap. **82**: 60–71. doi:10.1016/j.dsr.2013.07.013

Siegel, D. A., K. O. Buesseler, S. C. Doney, S. F. Sailley, M. J. Behrenfeld, and P. W. Boyd. 2014. Global assessment of ocean carbon export by combining satellite observations and food-web models. Global Biogeochem. Cycles **28**: 181–196. doi:10.1002/2013GB004743

Silver, M. W., and K. W. Bruland. 1981. Differential feeding and fecal pellet composition of salps and pteropods, and the possible origin of the deep-water flora and olive-green "Cells." Mar. Biol. **62**: 263–273. doi:10.1007/BF00397693

Smayda, T. J. 1970. The suspension and sinking of phytoplankton in the sea. Oceanogr. Mar. Biol. Annu. Rev. **8**: 353–414. doi:10.1002/iroh.19720570110

Smayda, T. J. 1971. Normal and accelerated sinking of phytoplankton in the sea. Mar. Geol. **11**: 105–122. doi:10.1016/0025-3227(71)90070-3

Smetacek, V. S. 1985. Role of sinking in diatom life-history cycles: Ecological, evolutionary and geological significance. Mar. Biol. **84**: 239–251. doi:10.1007/BF00392493

Trull, T. W., S. G. Bray, K. O. Buesseler, C. H. Lamborg, S. Manganini, C. Moy, and J. Valdes. 2008. In situ measurement of mesopelagic particle sinking rates and the control of carbon transfer to the ocean interior during the Vertical Flux in the Global Ocean (VERTIGO) voyages in the North Pacific. Deep-Sea Res. Part II Top. Stud. Oceanogr. **55**: 1684–1695. doi:10.1016/j.dsr2.2008.04.021

Volk, T., and M. Hoffert. 1985. Ocean carbon pumps: Analysis of relative strengths and efficiencies in ocean-driven atmospheric CO2 changes. Geophys. Monogr. Ser. **32**: 99–110. doi:10.1029/GM032p0099

Waite, A., P. K. Bienfang, and P. J. Harrison. 1992a. Spring bloom sedimentation in a subarctic ecosystem. I. Nutrient sensitivity. Mar. Biol. **114**: 119–129. doi:10.1007/BF00350861

Waite, A., P. K. Bienfang, and P. J. Harrison. 1992b. Spring bloom sedimentation in a subarctic ecosystem. II. Succession and sedimentation. Mar. Biol. **114**: 131–138. doi:10.1007/BF00350862

Waite, A. M., K. A. Safi, J. A. Hall, and S. D. Nodder. 2000. Mass sedimentation of picoplankton embedded in organic aggregates. Limnol. Oceanogr. **45**: 87–97. doi:10.4319/lo.2000.45.1.0087

Waite, A. M., and S. D. Nodder. 2001. The effect of in situ iron addition on the sinking rates and export flux of Southern Ocean diatoms. South. Ocean Iron Release Exp. SOIREE **48**: 2635–2654. doi:10.1016/S0967-0645(01)00012-1

Wiedmann, I., M. Reigstad, A. Sundfjord, and S. Basedow. 2014. Potential drivers of sinking particle's size spectra and vertical flux of particulate organic carbon (POC): Turbulence, phytoplankton, and zooplankton. J. Geophys. Res. Oceans **119**: 6900–6917. doi:10.1002/2013JC009754

Wilson, S. E., D. K. Steinberg, and K. O. Buesseler. 2008. Changes in fecal pellet characteristics with depth as indicators of zooplankton repackaging of particles in the mesopelagic zone of the subtropical and subarctic North Pacific Ocean. Deep-Sea Res. Part II Top. Stud. Oceanogr. **55**: 1636–1647. doi:10.1016/j.dsr2.2008.04.019

Young, J. R., M. Geisen, and I. Probert. 2005. A review of selected aspects of coccolithophore biology with implications for paleobiodiversity estimation. Micropaleontology **51**: 267–288. doi:10.2113/gsmicropal.51.4.267

Zar, J. 1999. Biostatistical analysis. Prentice Hall.